

Studying vascular smooth muscle cell characteristics using an alternating-substrate modulus system

Honors Thesis

Austin Becicka

Spring 2015

Advisor: Patrick Alford, PhD

Abstract

Cardiovascular diseases resulting from atherosclerosis comprise the single biggest cause of death in the developed world¹. In atherosclerosis, both local vessel stiffness and extracellular organization is perturbed. Vascular smooth muscle cell (VSMC) function is perturbed in atherosclerosis, but it is not clear if this is due to the evolving changes in extracellular mechanical stimuli. Here, we will build upon previous work using microfabrication techniques to determine the influence of extracellular matrix (ECM) mechanics and ECM organization on VSMC self-organization. We will use our previously developed alternating-substrate modulus system combined with microcontact printing (MCP) to observe and quantify cell self-organization when cells are guided by both the stiffness of the underlying substrate and stamped lines of fibronectin protein. This study will provide insight on VSMC behavior with competing influences on cell self-organization and may help provide insight to cell characteristics that may be useful in developing atherosclerosis therapies.

Introduction

Cardiovascular diseases caused by atherosclerosis comprise the number one cause of death in the developed world, accounting for one out of every three adult deaths¹. Atherosclerosis lesions consist of asymmetric thickenings of the tunica intima (Fig. 1). They consist of cells, connective-tissue elements, lipids, and other cellular debris². Atherosclerosis can develop in response to vessel wall injury caused by many stimuli including diabetes and hypertension. After initial injury, many cell types, including vascular smooth muscle cells (VSMCs), platelets, and inflammatory cells release growth factors and cytokines that lead to multiple effects. The released factors promote the transition of VSMCs from a quiescent contractile state to the active synthetic state, VSMC migration and proliferation, and extracellular matrix (ECM) protein deposition^{2,3}. VSMCs transition from quiescent to synthetic marks a key step in atherosclerosis disease progression, yet its cause remains poorly understood.

In the native vessel, VSMCs are surrounded by a highly structured ECM consisting of collagens type I and III, elastin, and proteoglycans. These molecules are important for maintaining tissue structure and play key roles in guiding cell function. Matrix metallo proteinases (MMPs) are enzymes thought to play a role in VSMC migration by catalyzing and removing the basement membrane around VSMCs and facilitating contacts with the surrounding interstitial matrix. Some research suggests that MMPs facilitate the transition of VSMCs from quiescent contractile to active synthetic.

Rigidity sensing plays an integral role in determining cellular behavior. Researchers have demonstrated that cells respond to the stiffness of their substrate by altering cytoskeletal organization, focal adhesions, and other processes that govern cell behaviors⁴. Cells grown on softer substrates have been shown to contain irregularly shaped, dynamic focal adhesions, while cells grown on stiffer

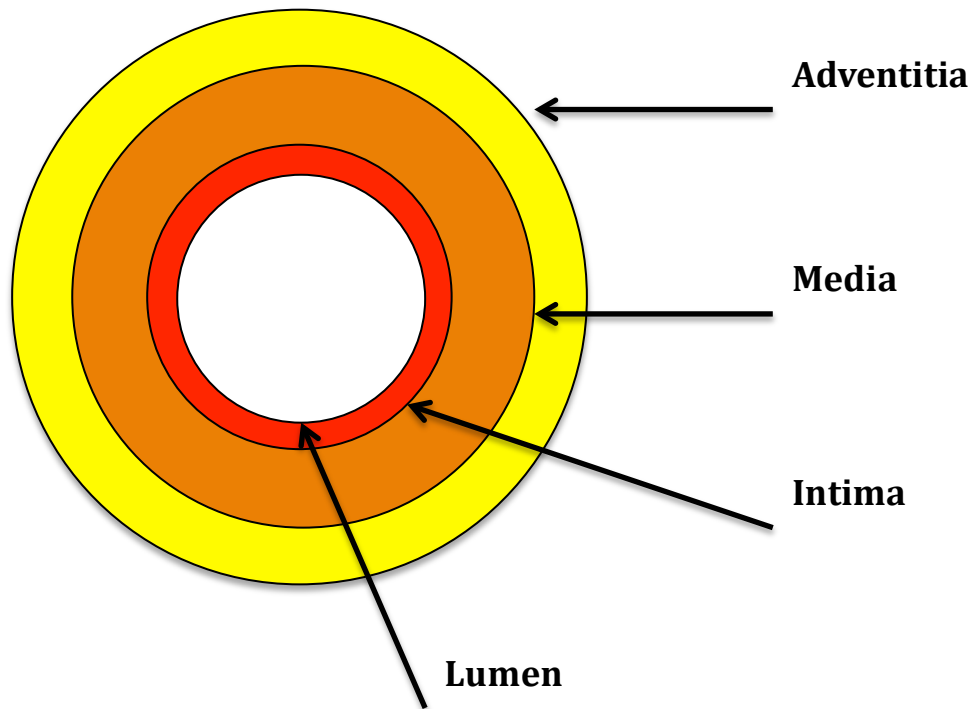


Fig. 1 The structural anatomy of arterial tissue in humans. VSMCs typically exist in the tunica media under normal conditions but can migrate to the tunica intima during a key step in progression of atherosclerosis.

substrates have been shown to be more stable⁵. Changes to the stiffness of the arterial wall that accompany vascular disease such as atherosclerosis are well established. For example, the elastic modulus of a normal vessel is 30 kPa but for a diseased vessel, the modulus of elasticity increases to 80 kPa⁶. Studies have shown cells respond to mechanical changes in their environment. Stem cells grown on stiffer substrates tend to develop distinct characteristics from cells grown on softer substrates⁷. Durotaxis was first coined by Lo et al. to describe the preferential migration of cells towards stiff substrates and away from soft substrates. Lo et al. determined that cells could detect substrate stiffness through tactile exploration via exerting a force on a new surface and measuring the resulting deformation⁸ (Fig. 2).

To date, it is unclear whether structural or mechanical changes are more important and how they change the key function of VSMCs: contractile stress generation. Previous studies have shown that cells can sense through soft substrates and exhibit different morphologies as the thickness of the soft substrate is altered⁹. Here, we develop an alternating-modulus substrate system using Polydimethylsiloxane (PDMS) composed of a stiff basement layer covered by a softer top layer. Using this system will be advantageous over previous systems because it can easily be adapted to measure VSMC contractility as done in previous studies.

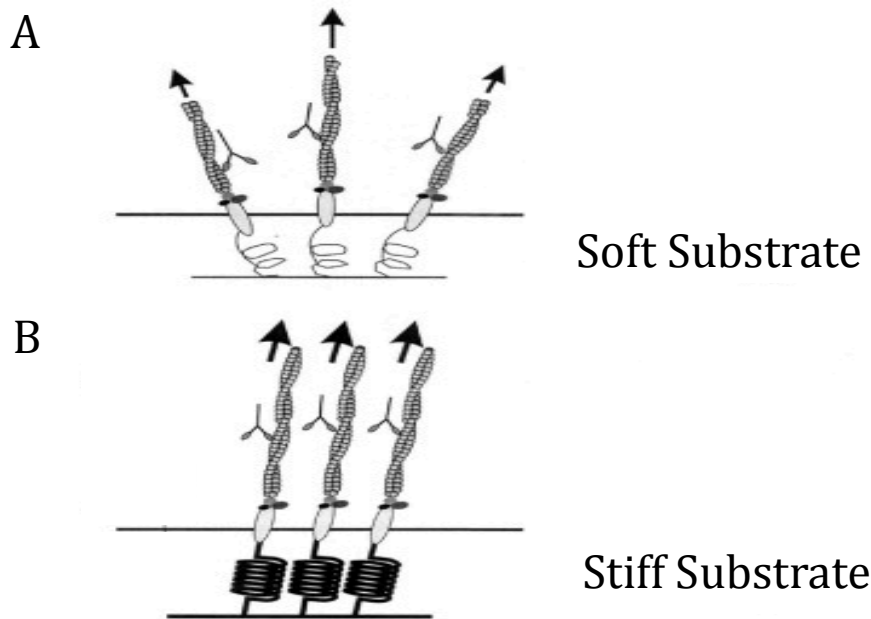


Fig. 2 A spring model for sensing mechanical stiffness proposed by Lo et al. showing actin probes interacting with the substrate via focal adhesions. (A) A low stiffness substrate does not provide a large resistance to pulling actin probes. **(B)** High stiffness substrate resists cell probes⁸.

Fibronectin is an ECM protein that mediates a variety of cellular interactions between the cell and its environment. Interactions between cells with the ECM through proteins such as fibronectin are important in regulating cell self-assembly. The ability to pattern ECM proteins such as fibronectin onto substrates is important for studying the complexities of the extracellular environment. Using soft photolithography methods, polydimethylsiloxane (PDMS) stamps with microfeatures are created and can be used to stamp fibronectin using MCP¹⁰. Previous studies have shown that using micropatterning approaches can be used to regulate cellular architecture.^{11,12} VSMCs have been shown to align preferentially along printed lines of fibronectin¹⁰. Furthermore, the functional contractile behavior of VSMCs is affected by cell shape, which can be manipulated with MCP to align and adhere to microcontact printed patterns in predictable ways.

Methods

Creating alternating-modulus substrate constructs

A silicon wafer was created with microscale-raised features (10 μm width lines, 20 mm long, and 10 μm apart) at the University of Minnesota nanofabrication center. The master was silanized overnight in a vacuum desiccator. Sylgard 184 polydimethylsiloxane (PDMS, Dow Corning) was used to mold devices from the master. PDMS at a 10 : 1 ratio of base : catalyst was poured onto the master and allowed to cure overnight at 90 °C. The PDMS was cut into 15 x 15 mm squares and silanized. The stamps were placed feature-side up and a drop of 184 10:1 ratio of base : catalyst PDMS was placed on each stamp and a 25 mm glass coverslip placed on top. The construct was placed in an oven and allowed to cure at 90 °C overnight. The glass coverslip was removed from the stamp to expose the 184 stiff layer adhered to the 25 mm glass coverslip. A mixture containing Sylgard 527 PDMS Part A and Part B in a 1:1 ratio was spin-coated on the 184 constructs at 3000 RPM for 60 seconds to create a thin layer and the construct was cured in an oven at 90°C overnight. The overall fabrication process is displayed in Fig. 3.

Cell culture

Human umbilical artery vascular smooth muscle cells (VSMCs) were purchased from Lonza at passage 3 and cultured at 37 °C and 5% CO₂ in a growth medium consisting of Medium 199 (GenDEPOT, Baker, TX) supplemented with 10% fetal bovine serum (Gibco, Grand Island, NY), 10 mM HEPES (Gibco), 3.5 g L⁻¹ glucose (Sigma-Aldrich, St. Louis, MO), 2 mg L⁻¹ vitamin B12 (SigmaAldrich), 50 U mL⁻¹ penicillin–streptomycin (Gibco), 1 x MEM non-essential amino acids (Gibco), and 2 mM L-glutamine (Gibco). All experiments were conducted at passages 5–7.

Microcontact printing

Extracellular matrix (ECM) protein fibronectin (FN, BD Biosciences, San Jose, CA) was microcontact printed on a PDMS substrate using standard techniques¹⁰. Stamps were cleaned by sonication in 70% ethanol for 30 m. The FN solution (50 $\mu\text{g mL}^{-1}$) was incubated on a PDMS stamp for 1 h then blown dry. This was done using both flat stamps and traditional lined stamps depending on the experiment. The alternating-modulus PDMS substrate was exposed to UV ozone for 8 m and the stamps were placed in conformal contact with the substrate, transferring the protein. Slight pressure was applied to the stamp then the stamps were peeled away, leaving the micropatterned protein.

Cell Seeding

VSMCs were trypsinized using 0.25% trypsin with EDTA (Invitrogen, Carlsbad, CA) and centrifuged at 200 relative centrifugal force for 5 m. After centrifuging the detached cells into a pellet, cells were resuspended and seeded on the constructs at a cell density of 49,000 cells per cm² construct surface area. The constructs were allowed to incubate overnight in growth medium. The tissues were serum-starved for 24 h to induce a contractile phenotype¹³.

Histochemistry

Tissues were fixed using 4% paraformaldehyde (Electron Microscopy Sciences, Hardfield, PA) for 5 m then stained for F-actin (Alexa Fluor 488 Phalloidin, Life Technologies) and nuclei (DAPI, 40,6-diamidino-2-phenylindole, Life Technologies). Stained tissues were imaged using an Olympus X-81 fluorescent microscope at 20 x magnification. F-actin and nuclei images were obtained by capturing ten random fields of view in a single tissue and three tissues per condition. Seeding density was calculated by quantifying the number of nuclei per area. Tissue alignment was analyzed using F-actin and nuclei images. Orientational order parameter (OOP) for each tissue construct was calculated using a Matlab program for actin fiber and nuclei orientation where an OOP of 1 indicates anisotropic alignment and an OOP of zero indicates isotropic alignment within the tissue. Nuclear shape was analyzed by fitting an ellipse to each nucleus.

Surface characterization

A P10 Tencor profilometer (KLA Tencor) in the Characterization Facility was used to characterize the surface of the alternating-modulus substrates created at various spin speeds and surface thicknesses. The P10 is capable of 0.5-angstrom vertical resolution. All samples with a soft PDMS surface (5kPa or less) was sputtercoated using a Cressington 208 sputter coater with gold before dragging the stylus across the surface to ensure that the construct did not break the stylus. Each sample was loaded into the profilometer separately and the stylus was dragged orthogonally to the patterned lines across 13 mm of the construct at a sampling rate of 4 data points per 1 μ m. The raw data was processed using Matlab. The process of analyzing data in Fourier space to reveal surface characteristics is outlined in Fig. 5. The calculation shown in Appendix A reveals that a result of approximately 65 index units corresponds to the 10 x 10 micron pattern of the underlying substrate. However, if the patterned lines of the underlying substrate were positioned at some angle with respect to the stylus the frequency would become lower than 65 index units. To correct for this, a range of frequencies from 40-70 index units was examined and the maximum signal over this range taken when calculating the SNR (Appendix B).

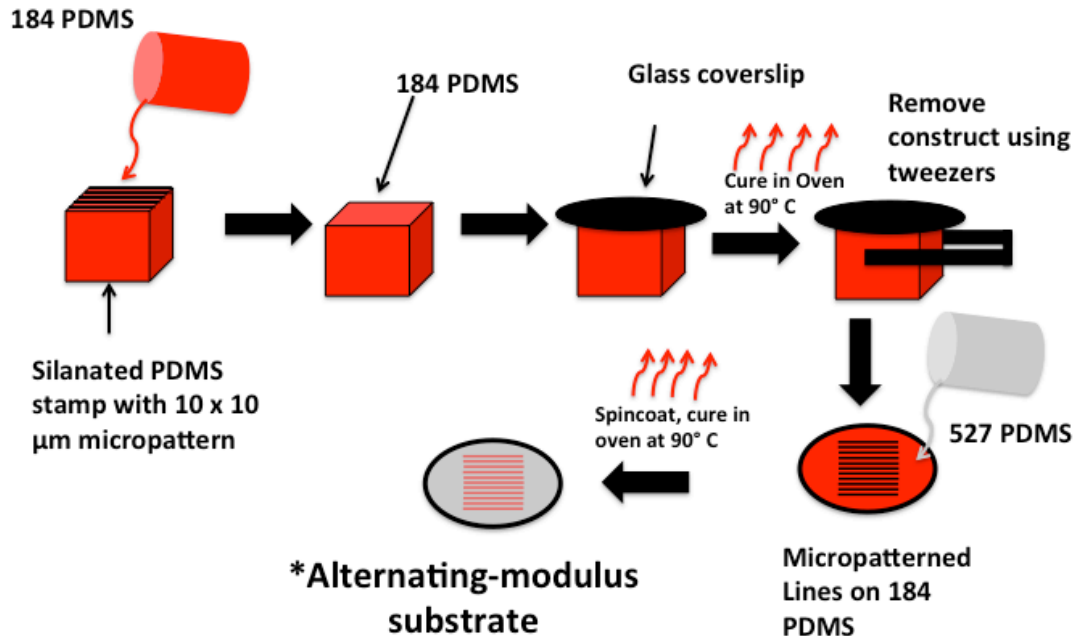


Fig 3. Construction of the alternating-modulus substrate constructs. First, 184 PDMS was placed on the silanated stamps with 10 x 10 μm microgrooves and a 25 mm glass coverslip placed on top of the PDMS. The stamp was cured in an oven at 90° C for 24 hours. The construct was removed from the stamp to reveal a glass coverslip with 10 x 10 μm microgrooves as shown. 527 PDMS was placed on the micropatterned lines followed by spincoating at 3000 RPM. The construct was cured in an oven at 90° C for 24 hours.

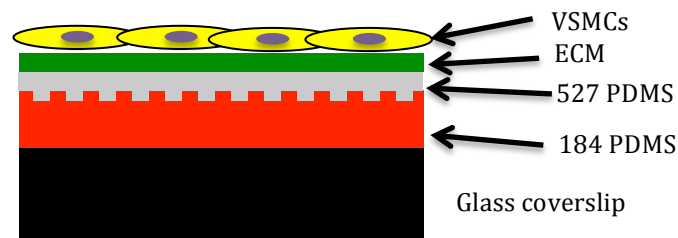


Fig. 4 A diagram of the fabricated alternating-modulus substrate. The 527 PDMS layer both fills in the gaps and creates a thin layer through which cells must sense. Fibronectin ECM is patterned on top of the 527 layer to provide attachment points for seeded VSMCs.

Results

Fabrication of the alternating substrate-modulus constructs

Previous studies have constructed an alternating-modulus substrate using two different types of polyethylene glycol hydrogels for the soft and stiff layers¹⁴. Here, we aimed to create an alternating-modulus substrate PDMS system using 184 and 527 PDMS for the stiff and soft layers respectively. This system was chosen because it is compatible with MTFs used previously to measure contractility of VSMCs. After experimenting with several techniques, we settled with a reverse embossing technique to create a stiff 184 layer as shown in Fig. 3. The resulting construct was spin coated with 527 PDMS at 3000 RPM for 60 seconds to create a thin layer. This was done to fill in the gaps and create a thin PDMS layer through which cells can sense. The construct was cured in an oven for 24 hours at 90 °C.

Characterization of the constructs

This method was subject to a significant degree of noise, making it difficult to interpret the results directly. Instead, the raw data from the profilometer was uploaded to Matlab where it was passed through a fast Fourier transform and binned so that it reflected the power spectrum the profilometer data. It was calculated that a frequency of 65 index units correlated to the spacing of the peaks in the 10 μm x 10 μm micropatterns on the constructs (Appendix A).

Constructs were created at spin speeds ranging from 500 RPM – 6000 RPM with 527 PDMS on a 25 mm glass coverslip serving as the control. The raw data obtained from the profilometer was processed in Matlab. The power spectrum was analyzed for low frequency spikes in a range from 40-70 index units corresponding to the 65 index units frequency of the 10 μm lines as shown in Fig. 5 (Appendix B). A second set of identical constructs was created and seeded with VSMCs at 49,000 cells per cm^2 . The cells were fixed, stained, and imaged to determine the actin and nuclei OOP as shown in Fig. 6B. We believe a key region exists when the thin layer of PDMS is spincoated on at 3000 RPM where VSMCs align preferentially along the underlying substrate yet the constructs are relatively flat. A sudden increase in the SNR occurs between 3000 RPM and 4000 RPM (Fig. 6B). A cartoon depicting the general findings from the profilometer and cell data is shown in Fig. 6C.

Cell alignment behavior

Studies have shown that VSMCs will align along patterned fibronectin during cell seeding¹⁰. After it was determined that the constructs were likely flat and they preferentially aligned with the underlying substrate, we wanted to determine whether cells would preferentially align due to the underlying substrate or patterned ECM when presented with both influences.

The constructs were spun at 3000 RPM and patterned with ECM at varying degrees of alignment between the lines and patterned ECM ranging from parallel to orthogonal (Fig. 7A). The control construct was patterned with uniform fibronectin

to test the influence of the underlying substrate alone. Cell images of actin were taken to determine the degree of alignment on each construct (Fig. 7B). A rose plot of the mean actin alignment was created with the direction of the underlying substrate along the zero axis (Fig. 7C). The mean actin and nuclei OOP for VSMCs tested against the underlying substrate is shown in Fig. 8. The results suggest that VSMC behavior is more controlled by changes to the ECM compared to the underlying substrate when cells are presented with competing influences.

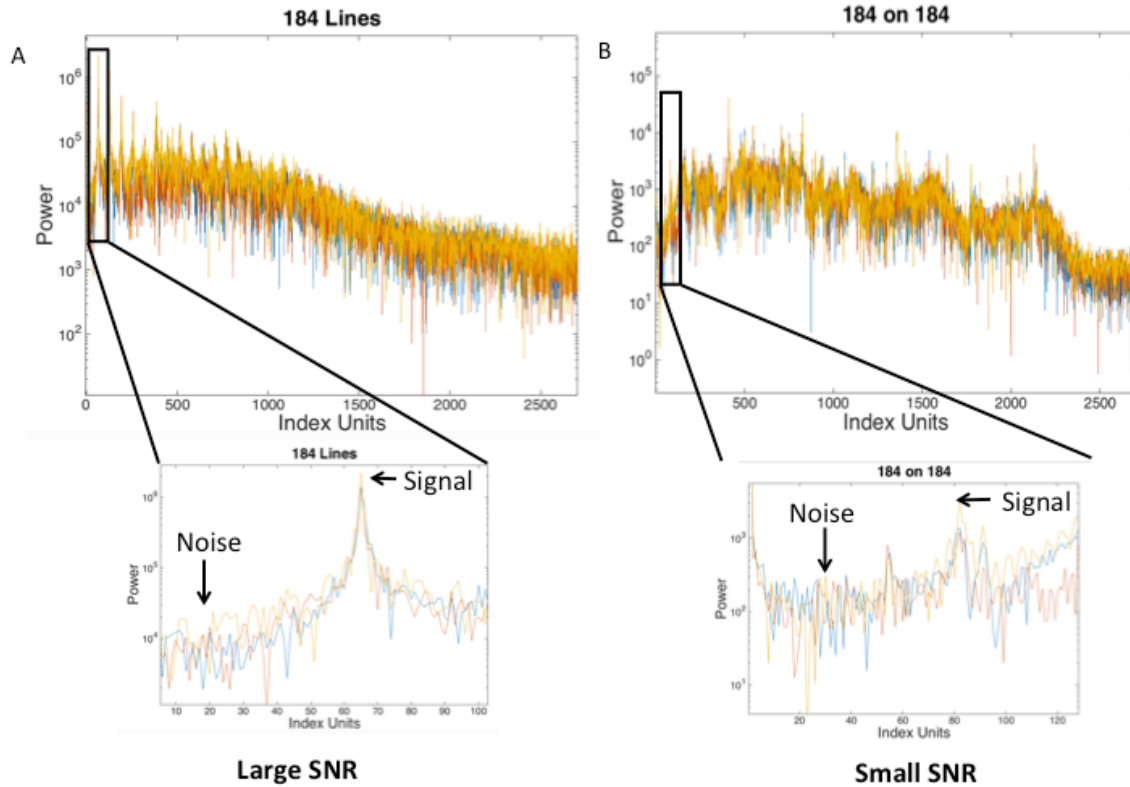


Fig. 5 Fourier analysis. (A) The power spectrum of the raw Fourier transform of the stiff 184 underlying substrate before spincoating the soft 527 layer. The yellow, red, and blue lines correspond to trials 1-3 respectively. The blowup shows the peak signal and mean noise used in code from Appendix B. The SNR will be large for this construct. (B) The power spectrum and blowup from a construct with a thick 2 mm layer of 184 PDMS patterned on top of the underlying substrate. The blowup does not show any significant peaks and the SNR will be small for this construct.

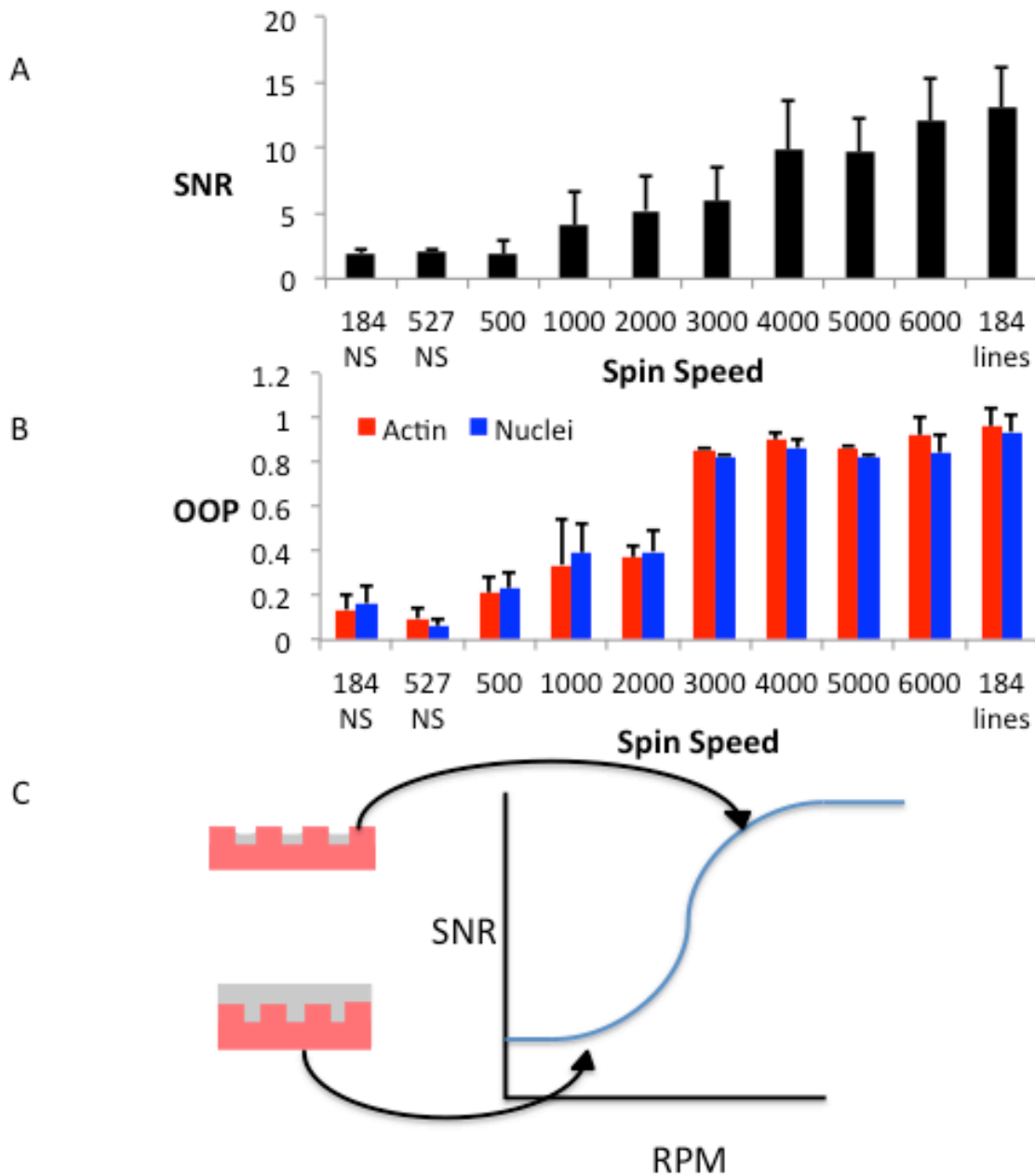


Fig. 6 The SNR reveals surface characteristics of the alternating modulus substrate. (A) A plot of the mean signal to noise ratio (SNR) versus spin speed of the spin coater used to spin the 527 PDMS layer atop the 184 PDMS layer (n=4). (B) The actin OOP for VSMCs seeded on the constructs obtained using confocal microscopy (n=2). (C) A cartoon illustration of surface topography for the 527 PDMS layer spun at low spin speed (bottom) and high spin speed (top).

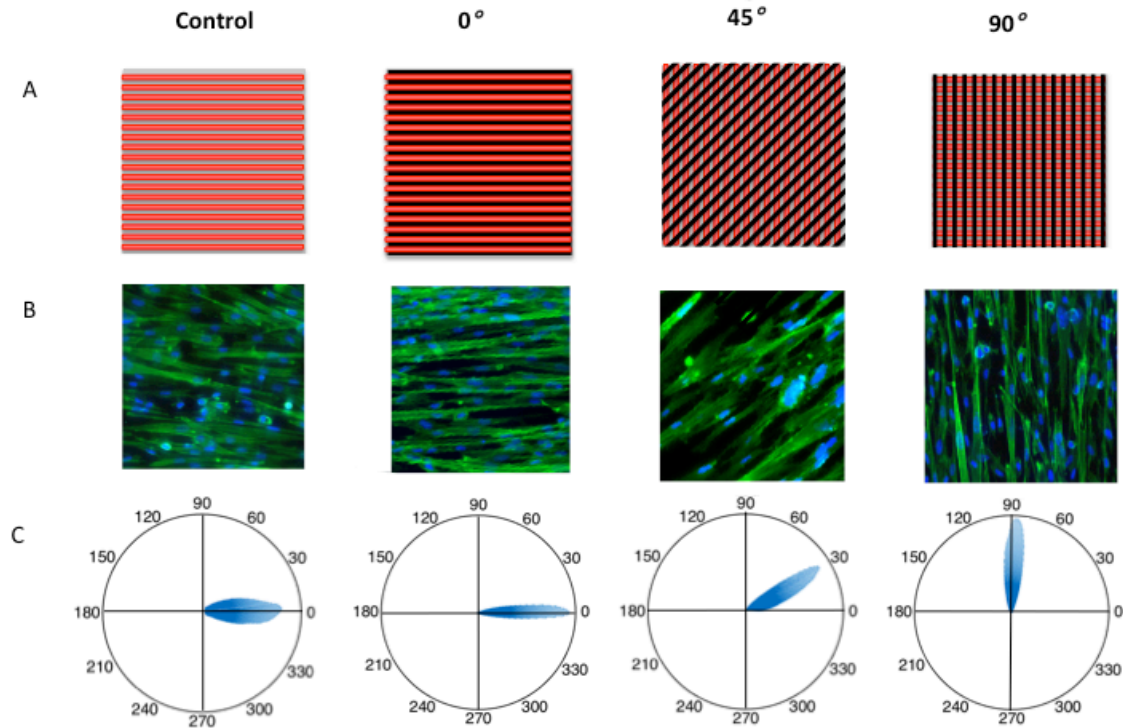


Fig. 7 The effect of competing influences on alternating-substrate modulus on cell alignment (A) The alternating-modulus construct consisting of alternating grey and red lines of 184 “stiff” PDMS and 527 “soft” PDMS respectively. Fibronectin is shown in black. The control was patterned with uniform fibronectin. Constructs were patterned at varying degrees of alignment relative to the lines of the construct. (B) Cell images taken in bright field showing the cells degree of alignment with the underlying substrate. (C) The degree of alignment of the mean actin alignment plotted on a rose plot where the constructs are at zero degrees (n=3).

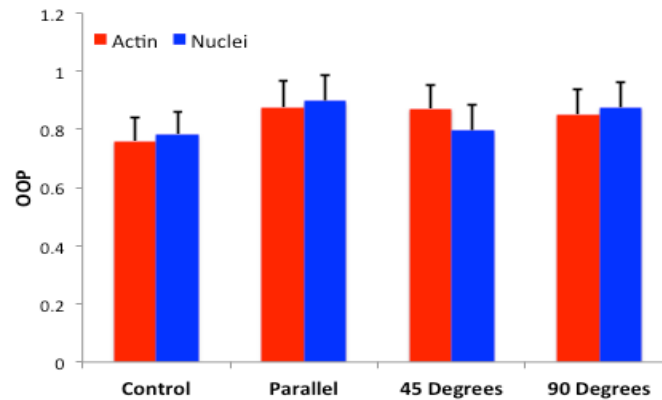


Fig. 8 The mean OOP for the various alignment patterns tested. The control was patterned with uniform fibronectin to assess the influence of the underlying substrate. Fibronectin patterned on 10 x 10 micron lines at varying degrees of alignment with the underlying substrate were patterned, seeded with cells, and fixed and stained. Nuclear and actin alignment was measured for each degree of alignment (n=3).

Discussion

Previously it was found that cells preferentially align with stiff substrates over soft substrates when patterned directly on an alternating stiff-soft hydrogel surface¹⁴. A previous study also found that mesenchymal stem cells (MSCs) were capable of sensing $\sim 10\ \mu\text{m}$ through a soft substrate (1 kPa) to detect the stiffer underlying glass substrate⁹. Here, we created alternating $10\ \mu\text{m}$ lines with stiff PDMS (184 Dow Corning, $\sim 1.5\ \text{MPa}$) covered with soft PDMS (527 Dow Corning, $\sim 5\ \text{kPa}$). We hypothesized that this system could be made using stiff and soft PDMS and cells would be able to sense and preferentially align with the underlying substrate through a thin layer of soft 527 PDMS. We successfully created an alternating substrate modulus system using two types of PDMS to provide the soft and stiff layer (Fig. 4.). We characterized these constructs using a profilometer to screen for grooves on the construct surface. Our results suggest that the constructs change from flat to grooved as the spin speed of the 527 layer changes from 3000 RPM to 4000 RPM. Constructs spun at spin speeds of 4000 RPM and above showed a higher SNR compared to lower spin speeds (Fig. 6A). However, cell experiments using the same constructs showed that cells begin to preferentially align at 2000 RPM before the SNR ratio reaches a plateau around 4000 RPM (Fig. 6B). Together, this suggests that there exists a spin speed range where cells align due to the sensing of the stiff underlying substrate before the formation of microgrooves.

Fig. 6A shows that the SNR did begin to increase for spin speeds ranging from 1000 RPM – 3000 RPM. This suggests that some grooves could have started to form in this range, potentially affecting cell alignment behavior. However, there was a noticeable increase in SNR between 3000 RPM and 4000 RPM suggesting that grooves were not fully formed until the 4000 RPM and above spin range. In further studies we plan to further characterize the surface properties of the alternating-modulus constructs using scanning electron microscopy to confirm surface properties.

After showing that cells preferentially aligned with the underlying substrate, we wanted to know whether the patterned ECM or underlying substrate had a greater influence on cell alignment. We did this by stamping fibronectin at varying degrees of alignment to the underlying substrate (Fig. 7A). We confirmed that the cells were feeling the underlying substrate by using a control patterned with uniform ECM. The actin and nuclei alignment showed that cells were highly aligned for all alignment scenarios tested (Fig. 8). Our results suggest that cells preferentially align much more with the patterned ECM compared to the underlying substrate (Fig 7B and Fig 7C). This may indicate that atherosclerotic treatments could be developed more easily that aim to prevent VSMC migration via controlling extracellular matrix production compared to controlling substrate stiffness.

This study revealed that an alternating substrate modulus system could be created with PDMS and used to reveal interesting insights into VSMC behavior. We were able to show that a sweet spot exists where cells align preferentially with the underlying substrate and constructs are flat. In future studies, we would assess cell contractility at a variety of degrees of alignment using vascular muscular thin films

(vMTFs) to determine whether the underlying substrate is capable of influencing contractility¹³. However, this protocol requires that the constructs be $\sim 10\ \mu\text{m}$ thin, which is not possible to attain using the fabrication method outlined in Fig. 3. We are currently pursuing a system that utilizes flowing PDMS through microfluidic devices to create the constructs at the appropriate thickness for fabrication of vMTFs.

Conclusion

Here, we created an alternating-modulus substrate system that provides insight into VSMC cell behavior under competing influences for alignment. Our results suggest a thickness range exists where cells can sense the underlying substrate yet the construct is relatively flat. Experiments with VSMCs showed that cells preferentially align with the patterned ECM over the underlying substrate when both influences are present. This result suggests that therapies aimed at controlling VSMC behavior via extracellular matrix production may be more viable compared to controlling vascular stiffness alone. In future studies we plan to further characterize this system using a thin film assay to assess VSMC contractility under competing influences on cell behavior as described in this paper.

Acknowledgements

I would like to thank Kerianne Steucke, Zaw Win, and Eric Hald for providing the training and expertise necessary for me to learn the techniques and data analysis cited in this paper. Parts of this work were carried out in the Minnesota Nano Center, which receives partial funding from NSF. Parts of this work were also carried out at the University of Minnesota Characterization Facility which receives funding from NIH and NSF.

Appendix

A: Target frequency calculation

In real space, 1291 μm is total distance stylus was dragged and stiff 184 lines are 10 μm apart.

We need to solve for the corresponding frequency of these lines in Fourier space

To do this, we will perform a simple calculation

Fs = sampling frequency = 4 samples/ micron

N = number of data points = 5164

L = distance between peaks = 20 microns

x = index frequency corresponding to 20 micron distance between points

Calculation:

$$x = \frac{N}{L * Fs} = \frac{5164 \text{ samples}}{20 \mu\text{m} * 4 \frac{\text{samples}}{\mu\text{m}}} = 64.55 \text{ index units}$$

x = 64.55 index units

B: Matlab Code used for Fourier Analysis

```
%Load data

load('3000A.TXT');
dX3000A = X3000A(:,1);
X3000A = X3000A(:,2);
load('3000B.TXT');
dX3000B = X3000B(:,1);
X3000B = X3000B(:,2);
load('3000C.TXT');
dX3000C = X3000C(:,1);
X3000C = X3000C(:,2);

%Plot data

figure
semilogy(abs(fft(diff(X3000A))))
hold all
semilogy(abs(fft(diff(X3000B))))
semilogy(abs(fft(diff(X3000C))))
title('3000', 'FontSize',14)
xlabel('Frequency (Index units)', 'FontSize',14)
ylabel('Power', 'FontSize',14)

%Calculate SNR ratio
A = abs(fft(diff(X3000A)));
B = abs(fft(diff(X3000B)));
```

```

C = abs(fft(diff(X3000C)));

%low frequency area of interest
A = A(40:70);
B = B(40:70);
C = C(40:70);

%Calculate SNR

SNR_A = max(A) / mean(A);
39 + find(A == max(A))

SNR_B = max(B) / mean(B);
39 + find(B == max(B))
SNR_C = max(C) / mean(C);
39 + find(C == max(C))
SNR_Data = [SNR_A; SNR_B ; SNR_C];
mean_SNR = mean(SNR_Data)

%Calculate standard deviation

std_SNR = std(SNR_Data)

```

References

- (1) World Health Organization 2015, *Fact Sheet N°317 – Cardiovascular Diseases*, <<http://www.who.int/mediacentre/factsheets/fs317/en/>>
- (2) Schaper W, Ito WD. Molecular mechanisms of coronary collateral vessel growth. *Circ Res*. 1996;79:911–9.
- (3) Wolf C, Cai WJ, Vosschulte R, et al. Vascular remodeling and altered protein expression during growth of coronary collateral arteries. *J Mol Cell Cardiol*. 1998;30:2291–305.
- (4) Califano, Joseph P., and Cynthia A. Reinhart-King. "Matrix Stiffness: A Regulator of Cellular Behavior and Tissue Formation." *Engineering Biomaterials for Regenerative Medicine Novel Technologies for Clinical Applications*. By Brooke N. Mason. N.p.: n.p., 2012. 19-31. Print.
- (5) Pelham, R. J., and YL. Wang. "Cell Locomotion and Focal Adhesions Are Regulated by Substrate Flexibility." *Proceedings of the National Academy of Sciences* 94.25 (1997): 13661-3665. Print.
- (6) Matsumoto T, Abe H, Ohashi T, Kato Y, Sato M. Local elastic modulus of atherosclerotic lesions of rabbit thoracic aortas measured by pipette aspiration method. *Physiol Meas*. 2002;23(4):635–648.
- (7) A. Engler, S. Sen, H. Lee Sweeney, D. E. Discher, Matrix Elasticity Directs Stem Cell Lineage Specification, *Cell*, Volume 126, Issue 4, 25 August 2006, Pages 677-689, ISSN 0092-8674.
- (8) Lo, Chun-Min, Hong-Bei Wang, Micah Dembo, and Yu-Li Wang. "Cell Movement Is Guided by the Rigidity of the Substrate." *Biophysical Journal* 79.1 (2000): 144-52. Web.
- (9) Buxboim A., Rajagopal K., Brown A. E. X., Discher D. E. (2010). How deeply cells feel: methods for thin gels. *J. Phys. Condens. Matter*. 22:194116 10.1088/0953-8984/22/19/194116
- (10) Alford, Patrick W., Alexander P. Nesmith, Johannes N. Seywerd, Anna Grosberg, and Kevin Kit Parker. "Vascular Smooth Muscle Contractility Depends on Cell Shape." *Integrative Biology* 3.11 (2011): 1063. Print.
- (11) C. S. Chen, M. Mrksich, S. Huang, G. M. Whitesides and D. E. Ingber, *Science*, 1997, 276, 1425–1428.
- (12) F. Y. McWhorter, T. Wang, P. Nguyen, T. Chung and W. F. Liu, *Proc. Natl. Acad. Sci. U. S. A.*, 2013, 110, 17253–17258.

- (13) P. W. Alford, A. W. Feinberg, S. P. Sheehy, K. K. Parker, Biohybrid thin films for measuring contractility in engineered cardiovascular muscle, *Biomaterials*, Volume 31, Issue 13, May 2010, Pages 3613-3621, ISSN 0142-9612
- (14) Diez, M., Schulte, V. A., Stefanoni, F., Natale, C. F., Mollica, F., Cesa, C. M., Chen, J., Möller, M., Netti, P. A., Ventre, M. and Lensen, M. C. (2011), Molding Micropatterns of Elasticity on PEG-Based Hydrogels to Control Cell Adhesion and Migration. *Adv. Eng. Mater.*, 13: B395–B404. doi: 10.1002/adem.201080122.